Heliyon 9 (2023) e21061

Contents lists available at ScienceDirect

Heliyon

journal homepage: www.cell.com/heliyon

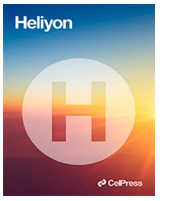

CIZ1 aggravates gastric cancer progression via mediating FBXL19-AS1 and miR-339-3p

Houmin Wan [a], Lianzhen Wang [a], Bin Huo [a], Zhongpeng Qiao [a], Yingli Zhang [b,*]

[a] Department of Gastrointestinal Surgery, The NO.4 Municipal Hospital Affiliated to Shandong First Medical University, Jinan, 250031, Shandong Province, China
[b] Department of Obstetrics, The NO.4 Municipal Hospital Affiliated to Shandong First Medical University, Jinan, 250031, Shandong Province, China

ARTICLE INFO

Keywords:
CIZ1
miR-339-3p
FBXL19-AS1
Gastric cancer

ABSTRACT

Gastric cancer (GC) remains a prevalent malignancy with high morbidity and mortality. CDKN1A interacting zinc finger protein 1 (CIZ1) has been demonstrated to have oncogenic functions in the development of cancers. We detected CIZ1 expression via quantitative real-time PCR (RT-qPCR). The protein level of CIZ1 was measured through Western blot. We noticed that CIZ1 expression was markedly enhanced in GC cells. Furthermore, functional experiments including colony formation assay, EdU staining assay, transwell assay, TUNEL staining assay and flow cytometry analysis uncovered that CIZ1 silencing attenuated cell malignant phenotypes in GC. Through bioinformatics tools and mechanism assays, we explored the up-stream mechanism of CIZ1 and determined that CIZ1 was modulated by FBXL19 antisense RNA 1 (FBXL19-AS1) and microRNA-339-3p (miR-339-3p). Additionally, miR-339-3p exerted a negative role on GC development in vitro, and FBXL19-AS1 depletion also had the inhibitory impacts on the progression of GC in vitro. Eventually, the finding that CIZ1 overexpression reversed the effects of FBXL19-AS1 silencing on GC development was validated by rescue assays. In a word, CIZ1 functioned as a tumor promoter in GC, indicating that CIZ1 might be a promising target for GC treatment.

1. Introduction

It is commonly acknowledged that gastric cancer (GC) is the fifth most frequent malignant cancers throughout the world [1]. The diagnosis of GC is often at an advanced stage with pathological processes such as malignant proliferation, extensive invasion and metastasis [2]. Gene targeted therapy for cancers has attracted increasing attention in recent years and underlying mechanisms behind gene therapy needs to be explored [3].

Long non-coding RNAs (lncRNAs) are validated to have close relationship with biological process of tumors. Da M et al. have revealed that lncRNA HOTAIR is high expressed in GC and predicts poor survival among GC patients [4]. Sun K et al. have reported that LINC00152 targets PRKAA1 to promote aerobic glycolysis in the process of GC [5]. Wu X et al. have verified that lncRNA BLACT1 contributes to GC resistance to oxaliplatin by sponging miR-361 to modulate ABCB1 [6]. Furthermore, FBXL19 antisense RNA 1 (FBXL19-AS1) impacts GC development through miR-876-5p/HMGB3 axis [7] or miR-431/ZEB1 axis [8].

Competing endogenous RNA (ceRNA) network has been studied as the hotpot when it comes to lncRNAs [9]. LncRNAs grab microRNAs (miRNAs) and competitively bind with miRNAs, releasing messenger RNAs (mRNAs) from binding to miRNAs [10]. For

* Corresponding author. The NO.4 Municipal Hospital, NO.52 Shifan Road, Jinan City, Shandong Province, China.
E-mail address: zouliangjiang07962@163.com (Y. Zhang).

https://doi.org/10.1016/j.heliyon.2023.e21061
Received 19 April 2023; Received in revised form 11 October 2023; Accepted 13 October 2023
Available online 14 October 2023

example, LINC00483 modulates cell proliferation and apoptosis in GC by regulating MAPKs in a ceRNA mode [11]. Lnc-ATB boosts GC progression via miR-141-3p/TGFβ2 axis [12]. In this research, we aim to explore the competing relationship between CIZ1 and FBXL19-AS1.

CIZ1 has been demonstrated to exert promoting functions in cancers including hepatocellular carcinoma [13] and bladder cancer [14]. The purpose of this paper is to unmask the influence of CIZ1 on GC progression.

2. Materials and methods

2.1. Cell lines

GC cell lines (AGS, HGC27 and MKN-45) and GES-1 (human gastric epithelial cell line) were procured from the Procell Life Science & Technology Co., Ltd., a company founded in Wuhan, China. Another GC cell (ECC10) was procured from QianNuo Biotechnology Co., Ltd (Hangzhou, China). AGS cells and HGC27/MKN-45/GES-1 cells underwent incubation in Ham's F-12 medium (Corning, Tewksbury, MA, USA) and RPMI-1640 medium respectively at 37 °C with 5 % CO_2. ECC10 cells were cultivated in DMEM (Corning). All these mediums contained 10 % FBS.

2.2. Cell transfection

ShRNAs specific to CIZ1 or FBXL19-AS1 were constructed by GenePharma, a biotech company registered in Shanghai, China. Gene overexpression was applied using pcDNA3.1 vector (Invitrogen) containing sequence of CIZ1. miR-339-3p mimics/miR-339-3p inhibitor, and their negative controls were also procured from GenePharma. The transfection of these plasmids was implemented via Lipofectamine 3000 (Invitrogen) for 48 h.

2.3. Quantitative real-time PCR (RT-qPCR)

Total RNAs of GC cells were isolated with the application of Trizol reagent (Takara, Otsu, Japan) in the light of manufacturer's descriptions. Then, the reverse transcription from RNAs to cDNAs was implemented via RevertAid First Strand cDNA Synthesis Kit (K1622, Thermo Fisher, IL, USA). Next, qPCR was conducted via GoTaq qPCR Master Mix (A6001, Promega, Madison, WI, USA). The fold changes of genes were determined using $2^{-\triangle\triangle CT}$. Triplicate was required for this assay. The qPCR primers designed in this study are shown in supplementary materials.

2.4. Colony formation assay

GC cells were cultured for 14 days in 6-well plates (1000 cells/well). Then, methanol was added into cell samples before adding 0.5 % crystal violet. Next, colonies were manually counted. Triplicate was required for this assay.

2.5. 5-Ethynyl-2′-deoxyuridine (EdU) assay

Transfected cells (3×10^4) were cultured in BeyoClick™ EdU Cell Proliferation Kit, supplied by Beyotime (Shanghai, China), for 2 h prior to adding DAPI dye for 5 min. Olympus fluorescence microscope (Carl Zeiss, Jena, Germany) was applied to assess EdU-positive cells. Assay was conducted in triplicate.

2.6. Transwell assays

Transwell assay was conducted to evaluate cell invasive or migratory ability by use of Transwell chambers (8-mm pore, 24-well, Corning) with Matrigel (BD Biosciences, Franklin Lakes, NJ, USA) pre-coating or not. 2×10^4 transfected cells were put into the upper chamber containing serum-free medium. In the meantime, the lower chamber was added with the medium containing serum. After fixation and staining, cells invaded or migrated to the lower chamber were counted. Triplicate was required for this experiment.

2.7. Transferase-mediated dUTP nick end labeling (TUNEL) assay

After paraformaldehyde fixation, cells were first cultured in terminal deoxynucleotidyl transferase (TdT) reaction cocktail, followed by Click-iT reaction cocktail treatment. DAPI was applied for the staining of nucleus. The fluorescence intensity was assessed under a fluorescence microscope. Triplicate was required for this assay.

2.8. Flow cytometry analysis

A total of 2×10^5 cells were treated with PBS twice. Detection of apoptosis cells was carried out via Annexin V-FITC/PI Apoptosis kit, supplied by Invitrogen. After staining for 15 min, this assay was implemented using FACSCalibur (BD Bioscience, San Jose, CA). Finally, the results were calculated using FlowJo software. Triplicate was required for this assay.

2.9. RNA pull down assay

This assay was implemented using Pierce Magnetic RNA-Protein Pull-Down Kit, supplied by Thermo Fisher (Waltham, MA), as guided by provider. Cell protein extracts were incubated using biotinylated miR-339-3p probes. The mixture recovered by magnetic beads was assayed by RT-qPCR. Triplicate was required for this assay.

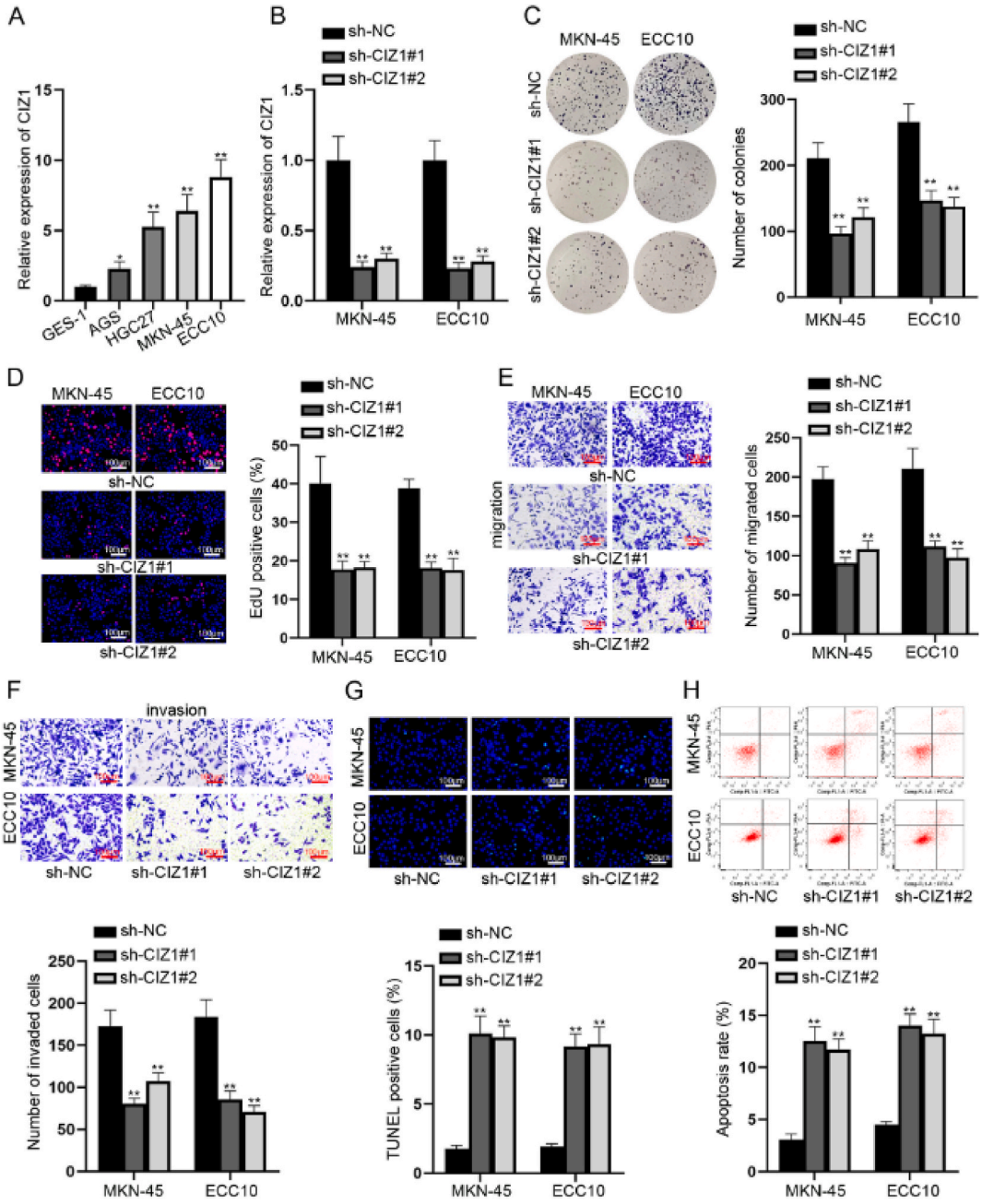

Fig. 1. CIZ1 is powerfully expressed in GC and contributes to GC progression in vitro. (A) The expression level of CIZ1 in GC cell lines and GES-1 cells was examined via RT-qPCR. (B) CIZ1 expression in MKN-45 and ECC10 cells was assessed through RT-qPCR after CIZ1 depletion. (C–D) Proliferation assays were implemented to measured GC cell proliferative ability after CIZ1 downregulation. (E–F) Cell migratory and invasive phenotypes were evaluated via transwell assay after CIZ1 silencing. (G–H) After CIZ1 knockdown, apoptosis experiments were implemented to detect the apoptotic rate of GC cells. *P < 0.05, **P < 0.01.

2.10. Luciferase reporter assay

After inserting wild-type (WT) or mutant-type (Mut) FBXL19-AS1 fragment or CIZ1 3′-UTR covering the miR-339-3p binding sites into pmirGLO (Promega), reporter plasmids were constructed, and transfected with miR-339-3p into GC cells. Next, the luciferase activity was evaluated with the application of Luciferase Reporter Assay System, supplied by Promega, with Renilla luciferase being internal reference. Assay was conducted in triplicate. The FBXL19-AS1 fragment sequence is in the supplemental material.

2.11. RNA-binding protein immunoprecipitation (RIP) assay

Cells cultured in 10 cm plate was washed twice with ice-cold PBS and scraped off in 1 mL PBS. Then the cell was centrifuged and re-suspended in an equal pellet volume of complete RIP lysis buffer from Magna RIP™ RNA-Binding Protein Immunoprecipitation Kit, supplied by MilliporeSigma (Bedford, MA, USA). 5 μg antibody was pre-bound to Protein A/G magnetic beads in immunoprecipitation buffer (20 mM Tris-HCl pH 7.5, 140 mM NaCl, 0.05 % TritonX-100) for 2 h and then incubated with 100 μl cell lysates over night at 4 °C with rotation. Then RNA was eluted from the beads by incubating with 400 μl elution buffer for 2 h. The eluted RNA was precipitated with ethanol and dissolved with RNase-free water. Enrichment of certain fragments was determined by qPCR.

2.12. Western blot

Total proteins of GC cells were acquired in RIPA buffer, and then analyzed by 12 % SDS-PAGE. Next, the isolated proteins were shifted to PVDF membranes and sealed in defatted milk. Secondary antibodies which were tagged by HRP and primary antibodies were

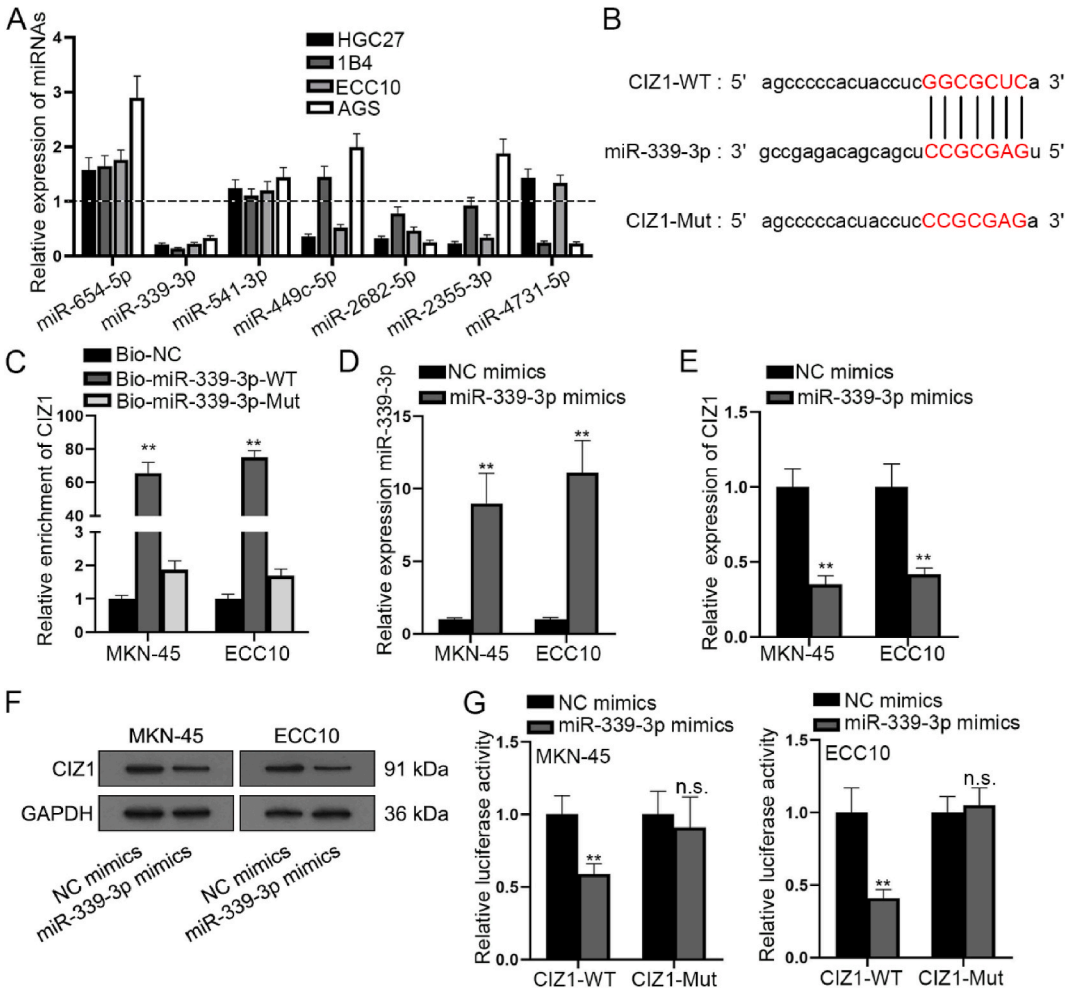

Fig. 2. MiR-339-3p binds to CIZ1 in GC cells. (A) The levels of candidate miRNAs in GC cell lines were detected. (B) ENCORI was utilized to obtain the binding sites of CIZ1 and miR-339-3p. (C) The enrichment of CIZ1 was examined via RNA pull down assay. (D) MiR-339-3p over-expression efficiency was evaluated. (E–F) CIZ1 expression level and protein level were tested in GC cells after miR-339-3p was overexpressed. (G) Luciferase reporter assay verified that CIZ1 could combine with miR-339-3p. "n.s." means no significance. **P < 0.01.

also procured from Abcam and used as instructed. All protein blots were visualized with the application of ECL detection system (Bio-Rad, Hercules, CA).

2.13. Bioinformatics analysis

ENCORI database (http://starbase.sysu.edu.cn) was utilized for predicting the miRNAs of CIZ1 (CLIP-Data ≥5; Degradome-Data ≥1) and the possible lncRNAs of miR-339-3p (CLIP-Data ≥3; Pan-Cancer ≥2). Meanwhile, binding sites among genes CIZ1, miR-339-3p, and FBXL19-AS1 were also got from ENCORI database.

2.14. Statistical analysis

Data for all assays were displayed by mean ± standard deviation. Student's t-test (two groups) or one-way ANOVA (more than two groups) was applied for assessing statistical significance of group difference. Statistical analysis was determined with the help of GraphPad Prism 5.0 which was obtained from GraphPad Software, Inc., a company founded in La Jolla, CA, USA, and specified as P value < 0.05.

3. Results

3.1. CIZ1 is powerfully expressed in GC cells and contributes to GC progression in vitro

To study whether CIZ1 could affect the development of GC cells, we firstly detected its expression. It turned out that CIZ1 expression was strikingly high in GC cell lines, especially in MKN-45 and ECC10 cells (Fig. 1A). Therefore, these two cells were selected out for the subsequent assays. Then, the expression of CIZ1 was efficiently knocked down in MKN-45 and ECC10 cells transfected with

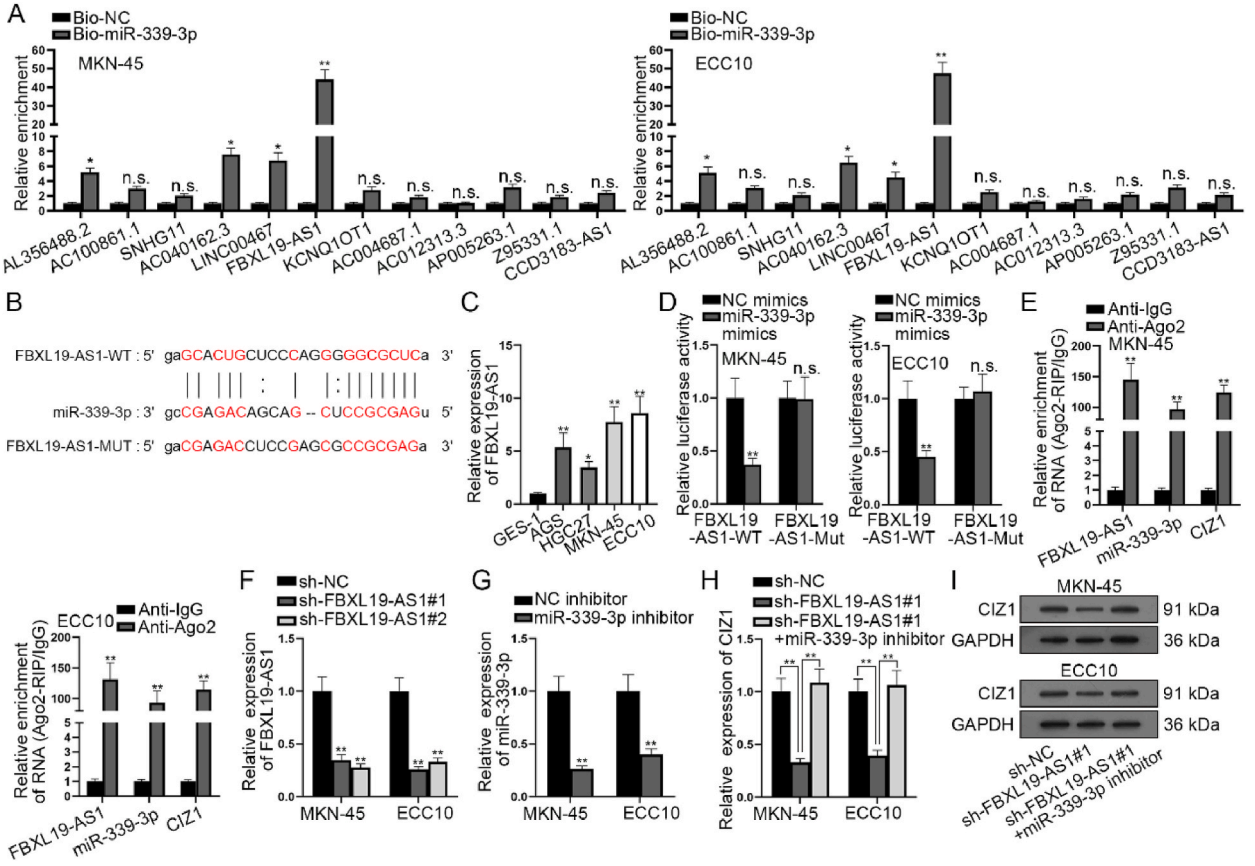

Fig. 3. FBXL19-AS1 targets miR-339-3p in GC. (A) The enrichment of candidate lncRNAs was measured via RNA pull down assay in GC cells. (B) ENCORI was utilized to obtain the binding sequences of FBXL19-AS1 and miR-339-3p. (C) FBXL19-AS1 expression in GC cells was assessed. (D) The activity of FBXL19-AS1-WT/MUT was examined by luciferase reporter assays. (E) RIP assays illustrated the relationship of CIZ1, miR-339-3p and FBXL19-AS1. (F) The efficiency of sh-FBXL19-AS1 was examined. (G) MiR-339-3p interference efficiency was tested. (H–I) The expression and protein level of CIZ1 were examined in different groups. "n.s." stands for no significance, *P < 0.05, **P < 0.01.

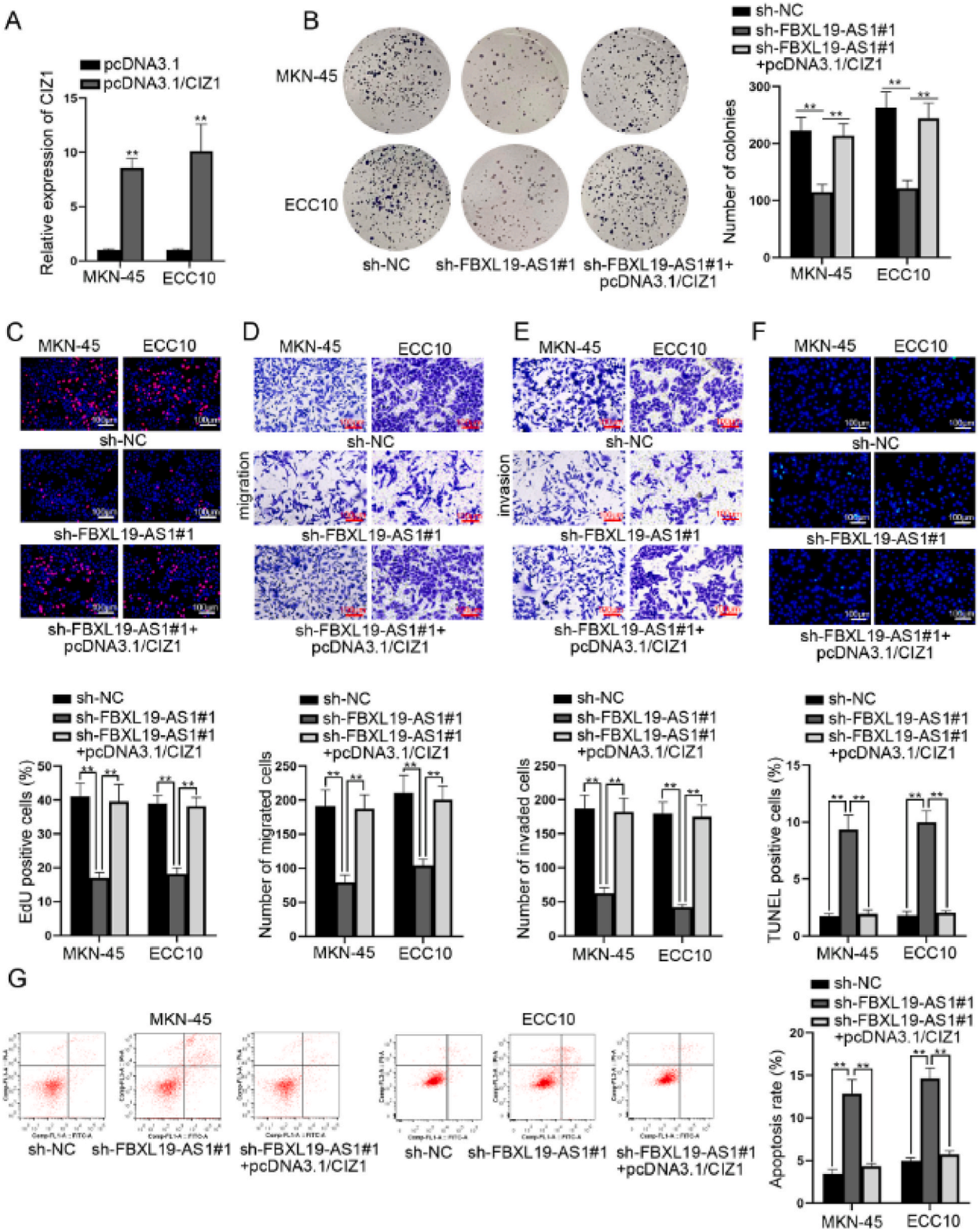

Fig. 4. FBXL19-AS1 exacerbates the progression of GC through targeting CIZ1. (A) The efficiency of CIZ1 overexpression was examined. (B–C) Cell proliferative phenotype was evaluated in different groups. (D–E) GC cell migratory and invasive phenotypes were measured under different transfections. (F–G) GC cell apoptosis was examined in different groups. **P < 0.01.

sh-CIZ1#1/2 (Fig. 1B). Proliferation assays demonstrated that reduction of CIZ1 inhibited the proliferative phenotype of MKN-45 and ECC10 cells (Fig. 1C–D). Likewise, cell migratory and invasive phenotypes were hampered by CIZ1 silencing (Fig. 1E–F). On the contrary, the apoptotic rate of GC cells was increased after CIZ1 silencing (Fig. 1G–H). Altogether, CIZ1 was markedly highly expressed in GC cells and promoted GC progression in vitro.

3.2. MiR-339-3p interacts with CIZ1

To probe the possible upstream mechanism of CIZ1, 7 possible miRNAs were predicted through the application of ENCORI database. Then, we uncovered that only miR-339-3p was markedly low-expressed in GC cells (Fig. 2A). Putative binding sites of miR-339-3p and CIZ1 were obtained (Fig. 2B). Furthermore, CIZ1 was significantly pulled down by biotinylated miR-339-3p (Fig. 2C). Furthermore, miR-339-3p expression levels were notably enhanced in MKN-45 and ECC10 cells after miR-339-3p overexpression (Fig. 2D). CIZ1 expression levels and protein levels in GC cells were found to be notably decreased when miR-339-3p expression was elevated (Fig. 2E–F). Then, we noticed that miR-339-3p augment declined the activity of CIZ1-WT (Fig. 2G). Moreover, we assessed the impact of miR-339-3p on GC progression. Firstly, up-regulation of miR-339-3p hindered cell proliferation in GC (Supplementary Figs. 1A–B). Meanwhile, the up-regulation of miR-339-3p alleviated GC cell migratory and invasive phenotypes (Supplementary Figs. 1C–D). Conversely, the cell apoptosis capacity was strengthened by up-regulation of miR-339-3p (Supplementary Figs. 1E–F). In short, miR-339-3p interacted with CIZ1 in GC cells and repressed the development of GC.

3.3. FBXL19-AS1 interacts with miR-339-3p in GC cells

It has been reported that LncRNAs can sequester miRNAs in ceRNA network. ENCORI database disclosed that there were 12 possible lncRNAs which could interact with miR-339-3p. Furthermore, we found that miR-339-3p had a strong binding affinity with FBXL19-AS1 among these lncRNAs (Fig. 3A). Putative binding sites of FBXL19-AS1 and miR-339-3p were shown in Fig. 3B. In addition, FBXL19-AS1 was markedly expressed in GC cells (Fig. 3C). Besides, the upregulation of miR-339-3p curbed the activity of FBXL19-AS1-WT but exerted no obvious influence on that of FBXL19-AS1-Mut (Fig. 3D). RIP assay further presented that the abundance of CIZ1, miR-339-3p and FBXL19-AS1 was notably high in Ago2 antibody groups (Fig. 3E). After the transfection of sh-FBXL19-AS1, FBXL19-AS1 expression was efficiently downregulated in MKN-45 and ECC10 cells (Fig. 3F). Similarly, miR-339-3p inhibitor was transfected to lessen miR-339-3p expression (Fig. 3G). Then, we found that the inhibition of FBXL19-AS1 knockdown on CIZ1 expression level and protein level was reversed by miR-339-3p silencing (Fig. 3H–I). Subsequently, the influence of FBXL19-AS1 knockdown on GC cells was evaluated as well. The data of cell proliferation assays suggested that depletion of FBXL19-AS1 ameliorated the proliferative phenotypes of GC cells (Supplementary Figs. 2A–B). Furthermore, FBXL19-AS1 silencing had suppressive impacts on cell migratory and invasive phenotypes (Supplementary Figs. 2C–D). In contrast, FBXL19-AS1 depletion induced cell apoptosis phenotype (Supplementary Figs. 2E–F). In conclusion, FBXL19-AS1 regulated miR-339-3p and contributed to GC progression.

3.4. FBXL19-AS1 exacerbates the progression of GC through targeting CIZ1

Eventually, to verify whether FBXL19-AS1 participated in the process of GC via modulation of CIZ1, rescue assays were implemented. After the transfection of pcDNA3.1/CIZ1, the expression of CIZ1 was strengthened in GC cells (Fig. 4A). Through cell proliferation assays, we found that the descending trend of cell proliferative phenotype caused by FBXL19-AS1 knockdown was completely counteracted by CIZ1 overexpression (Fig. 4B–C). Likewise, the suppression of FBXL19-AS1 silencing on cell migratory and invasive abilities was completely countervailed by CIZ1 overexpression (Fig. 4D–E). However, FBXL19-AS1 down-regulation stimulated the apoptosis of MKN-45 and ECC10 cells and such promotion was completely offset by overexpression of CIZ1 (Fig. 4F–G). In summary, FBXL19-AS1 promoted the progression of GC via enhancing CIZ1 expression.

4. Discussion

GC has been demonstrated to be the fifth most prevalent malignant cancer throughout the world and has high morbidity and mortality [1]. CIZ1 aggravates cell proliferation and migration in gallbladder cancer [15]. CIZ1 could facilitate the tumorigenicity of prostate carcinoma cells [16]. CIZ1 has also been reported to affect bladder cancer cell proliferation [14]. This research firstly uncovered that CIZ1 expression was notably enhanced in GC cells. Consistent with the previous studies [14], we uncovered that silencing of CIZ1 repressed the malignant phenotypes of GC cells. These findings revealed that CIZ1 was an oncogene in GC.

MiRNAs have been certified to have crucial functions in the process of human diseases [17]. For instance, miR-27b suppresses GC process via targeting NR2F2 [18]. MiR-616-3p contributes to angiogenesis and EMT process in GC cells through targeting PTEN/AKT mTOR pathway [19]. MiR-339-3p hinders cell proliferation by targeting Skp2 in lung cancer [20]. The former study has verified that miR-339-3p suppresses the tumorigenesis of melanoma [21]. In this research, we discovered that CIZ1 could interact with miR-339-3p. Moreover, we demonstrated the low-expressed of miR-339-3p in GC cells and its up-regulation retarded the progression of GC, which implied that miR-339-3p was an anti-oncogene in GC.

Inspired by ceRNA network, we focused on the lncRNAs which could bind with miR-339-3p. Through our investigation, we determined that FBXL19-AS1 had interaction with miR-339-3p in GC cells, and was highly expressed in GC cells. Moreover, functional assays further illustrated that FBXL19-AS1 inhibition could repress GC progression in vitro. Finally, the impacts of FBXL19-AS1 depletion on GC growth were counteracted by overexpression of CIZ1.

All in all, the data of our studies confirmed a novel ceRNA axis of FBXL19-AS1/miR-339-3p/CIZ1 in GC. The crucial role of CIZ1 in GC was revealed for the first time. Nonetheless, possible signaling pathways exist in the downstream of CIZ1 remains to be further explored. In addition, the screening of binding miRNAs of CIZ1 and candidate lncRNAs of miR-339-3p was performed under a variety of conditions. Therefore, other potential regulatory mechanisms in the process of GC also need further investigation. Besides, the impact of FBXL19-AS1/miR-339-3p/CIZ1 axis in GC was only verified in vitro. We intend to perform in vivo assays and clinicopathological analysis in the future to improve our understanding on GC treatment.

Data availability

The data that support the findings of this study are available from the corresponding author.

CRediT authorship contribution statement

Houmin Wan: Data curation, Formal analysis, Investigation, Methodology, Resources, Software, Supervision, Validation, Visualization, Writing – original draft, Writing – review & editing. **Lianzhen Wang:** Data curation, Formal analysis, Investigation, Methodology, Resources, Writing – original draft, Writing – review & editing. **Bin Huo:** Data curation, Resources, Writing – review & editing. **Zhongpeng Qiao:** Methodology, Supervision, Writing – review & editing. **Yingli Zhang:** Conceptualization, Formal analysis, Project administration, Resources, Software, Writing – original draft, Writing – review & editing.

Declaration of competing interest

The authors declare that they have no conflict of interest.

Appendix A. Supplementary data

Supplementary data to this article can be found online at https://doi.org/10.1016/j.heliyon.2023.e21061.

References

[1] H. Yoon, N. Kim, Diagnosis and management of high risk group for gastric cancer, Gut Liver 9 (1) (2015) 5–17.
[2] Y.J. Choi, N. Kim, Gastric cancer and family history, Korean J. Intern. Med. 31 (6) (2016) 1042–1053.
[3] Y. Jiang, Y. Yu, Transgenic and gene knockout mice in gastric cancer research, Oncotarget 8 (2) (2017) 3696–3710.
[4] M. Da, et al., High expression level of long non-coding RNA HOTAIR is associated with poor overall survival in gastric cancer patients: evidence from meta-analysis, J. BUON 22 (4) (2017) 911–918.
[5] K. Sun, P. Hu, F. Xu, LINC00152/miR-139-5p regulates gastric cancer cell aerobic glycolysis by targeting PRKAA1, Biomed. Pharmacother. 97 (2018) 1296–1302.
[6] X. Wu, et al., Long noncoding RNA BLACAT1 modulates ABCB1 to promote oxaliplatin resistance of gastric cancer via sponging miR-361, Biomed. Pharmacother. 99 (2018) 832–838.
[7] R.X. Ji, et al., LncRNA FBXL19-AS1 promotes the development of gastric cancer by regulating miR-876-5p/HMGB3 axis, J. Biol. Regul. Homeost. Agents 34 (4) (2020) 1513–1518.
[8] X.L. Wang, et al., Long non-coding RNA FBXL19-AS1 serves as a competing endogenous RNA to regulate ZEB1 expression by sponging miR-431 in gastric cancer, J. Biol. Regul. Homeost. Agents 34 (5) (2020) 1847–1855.
[9] G. Zhang, et al., LncRNA MT1JP functions as a ceRNA in regulating FBXW7 through competitively binding to miR-92a-3p in gastric cancer, Mol. Cancer 17 (1) (2018) 87.
[10] X.Z. Yang, et al., LINC01133 as ceRNA inhibits gastric cancer progression by sponging miR-106a-3p to regulate APC expression and the Wnt/beta-catenin pathway, Mol. Cancer 17 (1) (2018) 126.
[11] R. Yan, et al., MicroRNA-150-5p affects cell proliferation, apoptosis, and EMT by regulation of the BRAF(V600E) mutation in papillary thyroid cancer cells, J. Cell. Biochem. 119 (11) (2018) 8763–8772.
[12] K. Lei, et al., Lnc-ATB contributes to gastric cancer growth through a MiR-141-3p/TGFbeta2 feedback loop, Biochem. Biophys. Res. Commun. 484 (3) (2017) 514–521.
[13] J. Wu, et al., CIZ1 is upregulated in hepatocellular carcinoma and promotes the growth and migration of the cancer cells, Tumour Biol. 37 (4) (2016) 4735–4742.
[14] X. Chen, et al., CIZ1 knockdown suppresses the proliferation of bladder cancer cells by inducing apoptosis, Gene 719 (2019), 143946.
[15] D. Zhang, et al., CIZ1 promoted the growth and migration of gallbladder cancer cells, Tumour Biol. 36 (4) (2015) 2583–2591.
[16] T. Liu, et al., Ciz1 promotes tumorigenicity of prostate carcinoma cells, Front. Biosci. (Landmark Ed.) 20 (4) (2015) 705–715.
[17] A. Vishnoi, S. Rani, MiRNA biogenesis and regulation of diseases: an overview, Methods Mol. Biol. 1509 (2017) 1–10.
[18] Q. Feng, et al., miR-27b inhibits gastric cancer metastasis by targeting NR2F2, Protein Cell 8 (2) (2017) 114–122.
[19] Z.H. Wu, et al., MiR-616-3p promotes angiogenesis and EMT in gastric cancer via the PTEN/AKT/mTOR pathway, Biochem. Biophys. Res. Commun. 501 (4) (2018) 1068–1073.
[20] H. Ren, Y. Zhang, H. Zhu, MiR-339 depresses cell proliferation via directly targeting S-phase kinase-associated protein 2 mRNA in lung cancer, Thorac. Cancer 9 (3) (2018) 408–414.
[21] C.E. Weber, et al., miR-339-3p is a tumor suppressor in melanoma, Cancer Res. 76 (12) (2016) 3562–3571.